

ARTICLE

Coordinates over Complex Terrain in Atmospheric Model

Wen-Yih Sun^{1,2,3*}

1. Department of Earth, Atmospheric and Planetary Sciences, Purdue University, W. Lafayette, IN, 47907, USA

2. Department of Atmospheric Sciences, National Central University, Chung-Li, Taoyuan, 320, Taiwan

3. Institute for Space-Earth Environmental Research, Nagoya University, Nagoya, 464-8601, Japan

ARTICLE INFO

Article history

Received: 15 December 2020

Accepted: 28 December 2020

Published Online: 31 January 2021

Keywords:

Navier-Stokes equations

Cartesian

Curvilinear

Covariant

Contravariant

Terrain following

ABSTRACT

In the terrain following coordinate, Gal-Chen and Somerville^[1] and other proposed a vertical coordinate $\bar{z} \propto (z - z_{bottom}) / (z_{top} - z_{bottom})$ and constant spatial intervals of $\delta\bar{x}$ and $\delta\bar{y}$ along the other directions. Because the variation of $\delta\bar{x}$ and $\delta\bar{y}$ was ignored, their coordinate does not really follow the terrain. It fails to reproduce the divergence and curl over a complex terrain. Aligning the coordinate with real terrain, the divergence and curl we obtained from the curvilinear coordinate are consistent with the Cartesian coordinate. With a modification, the simulated total mass, energy, and momentum from the Navier-Stokes equations are conserved and in agreement with those calculated from Cartesian coordinate.

1. Introduction

Numerical atmospheric and oceanic models are usually applied over complex terrain^[2-10, etc.]. Hence, models require different coordinate to handle the irregular terrain. One of the terrain following coordinates, discussed in the papers^[1,5,11,12], has been applied to Regional Atmospheric Modeling System (RAMS)^[13], Geesthacht Simulation Model of the Atmosphere (GESIMA)^[11], Cloud Resolving Strom Simulator (CRess)^[7,14], Japan Meteorological Research Institute (MRI-model)^[5], WRF^[8], and other models. The relationship between their coordinates

$(\bar{x}, \bar{y}, \bar{z})$ and the Cartesian coordinates (x, y, z) satisfies:

$$\bar{x} = x, \bar{y} = y, \text{ and } \bar{z} = \frac{z_t(z - z_b)}{z_t - z_b},$$

where z_t and z_b are the height of the domain and the terrain elevation, respectively. This popular coordinate works well when it is applied to the gradient $\nabla\psi$, but it fails to produce the accurate divergence or the curl over a sloped mountain. It cannot be applied to the Navier-Stokes equations either. Although the coordinate is simple, it does not consider the variation of the spatial intervals over the terrain because $\delta\bar{x} = \delta x$, and $\delta\bar{y} = \delta y$. We propose a true terrain fol-

*Corresponding Author:

Wen-Yih Sun,

Department of Earth, Atmospheric and Planetary Sciences, Purdue University, W. Lafayette, IN, 47907, USA;

Department of Atmospheric Sciences, National Central University, Chung-Li, Taoyuan, 320, Taiwan;

Institute for Space-Earth Environmental Research, Nagoya University, Nagoya, 464-8601, Japan;

Email: wysun@purdue.edu

lowing coordinate, in which the spatial intervals are not constant but vary with the terrain. This system can accurately simulate the divergence and curl over a complex terrain. When it is applied to the Navier-Stokes equations with some modification, the total mass, energy and momentum calculated from the curvilinear coordinate are conserved and agree with those calculated from the Cartesian system.

2. Equations

2.1 General Curvilinear Coordinate

The detailed transformation between the Cartesian coordinate and the general curvilinear coordinate can be found in vector and tensor analysis books^[15,16], as well as research articles^[17,18]. In a curvilinear coordinate, a position vector (or any other vector) can be presented by

$$\mathbf{r} = \hat{x}^i \mathbf{g}_i (= \sum_1^3 \hat{x}^i \mathbf{g}_i) = \hat{x}_i \mathbf{g}^i (= \sum_1^3 \hat{x}_i \mathbf{g}^i) \quad (1)$$

where \mathbf{g}_i is the covariant basis vector along the curvilinear coordinate \hat{x}^i (a contravariant quantity), and the contravariant basis vector (or dual basis vector) \mathbf{g}^i ($i=1, 2, 3$), as shown in Figure 1. They satisfy:

$$\mathbf{g}_i \cdot \mathbf{g}^j = \delta_i^j \quad (2a)$$

$$\hat{x}_i = (\hat{x}_j \mathbf{g}^j) \cdot \mathbf{g}_i = \mathbf{r} \cdot \mathbf{g}_i; \quad \hat{x}^i = (\hat{x}^j \mathbf{g}_j) \cdot \mathbf{g}^i = \mathbf{r} \cdot \mathbf{g}^i \quad (2b)$$

and

$$\mathbf{g}^1 = \frac{\mathbf{g}_2 \times \mathbf{g}_3}{J}, \quad \mathbf{g}^2 = \frac{\mathbf{g}_3 \times \mathbf{g}_1}{J}, \quad \mathbf{g}^3 = \frac{\mathbf{g}_1 \times \mathbf{g}_2}{J}, \quad (2c)$$

$$J = \mathbf{g}_1 \cdot \mathbf{g}_2 \times \mathbf{g}_3 = \mathbf{g}_1 \times \mathbf{g}_2 \cdot \mathbf{g}_3 = \mathbf{g}_2 \times \mathbf{g}_3 \cdot \mathbf{g}_1 \quad (2d)$$

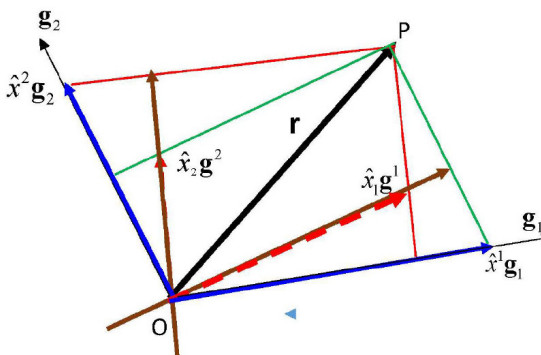


Figure 1. covariant basis vectors (\mathbf{g}_i), contravariant basis vectors (\mathbf{g}^i), and a 2D vector

$$\mathbf{r} = \hat{x}^1 \mathbf{g}_1 + \hat{x}^2 \mathbf{g}_2 = \hat{x}_1 \mathbf{g}^1 + \hat{x}_2 \mathbf{g}^2$$

In the Cartesian system, the basis vectors \mathbf{e}_i and the

change of the position vector satisfies:

$$d\mathbf{r} = \frac{\partial \mathbf{r}}{\partial x} dx + \frac{\partial \mathbf{r}}{\partial y} dy + \frac{\partial \mathbf{r}}{\partial z} dz = \mathbf{e}_x dx + \mathbf{e}_y dy + \mathbf{e}_z dz = \mathbf{e}_i dx^i \quad (3)$$

In the curvilinear system, it becomes

$$d\mathbf{r} = \frac{\partial \mathbf{r}}{\partial \hat{x}^i} d\hat{x}^i = \mathbf{g}_i d\hat{x}^i \quad (4a)$$

and the covariant basis vectors are

$$\mathbf{g}_i = \frac{\partial \mathbf{r}}{\partial \hat{x}^i} = \mathbf{e}_j \frac{\partial x^j}{\partial \hat{x}^i} = \mathbf{e}_x \frac{\partial x}{\partial \hat{x}^i} + \mathbf{e}_y \frac{\partial y}{\partial \hat{x}^i} + \mathbf{e}_z \frac{\partial z}{\partial \hat{x}^i} \quad (4b)$$

The gradient operator is

$$\nabla \equiv \mathbf{g}^i \frac{\partial}{\partial \hat{x}^i} = \mathbf{e}_i \frac{\partial}{\partial x^i} \quad (5a)$$

and

$$\nabla \hat{x}^i = \mathbf{g}^j \frac{\partial \hat{x}^i}{\partial \hat{x}^j} = \mathbf{g}^i = \mathbf{e}_j \frac{\partial \hat{x}^i}{\partial x^j} \quad (5b)$$

The Jacobian matrix is

$$J = [\mathbf{g}_1, \mathbf{g}_2, \mathbf{g}_3] = \det \left[\frac{\partial \mathbf{r}}{\partial \hat{x}^1}, \frac{\partial \mathbf{r}}{\partial \hat{x}^2}, \frac{\partial \mathbf{r}}{\partial \hat{x}^3} \right] = \det \begin{bmatrix} \frac{\partial x}{\partial \hat{x}^1} & \frac{\partial x}{\partial \hat{x}^2} & \frac{\partial x}{\partial \hat{x}^3} \\ \frac{\partial y}{\partial \hat{x}^1} & \frac{\partial y}{\partial \hat{x}^2} & \frac{\partial y}{\partial \hat{x}^3} \\ \frac{\partial z}{\partial \hat{x}^1} & \frac{\partial z}{\partial \hat{x}^2} & \frac{\partial z}{\partial \hat{x}^3} \end{bmatrix} \quad (6)$$

For a scalar variable S

$$dS = \frac{\partial S}{\partial \hat{x}^i} d\hat{x}^i = \mathbf{g}^j \frac{\partial S}{\partial \hat{x}^i} \cdot \mathbf{g}_k d\hat{x}^k = \mathbf{g}^j \frac{\partial S}{\partial \hat{x}^i} \cdot d\mathbf{r} = \nabla S \cdot d\mathbf{r} \quad (7)$$

where $\nabla S = \mathbf{g}^i \frac{\partial S}{\partial \hat{x}^i} = \mathbf{e}_i \frac{\partial S}{\partial x^i}$ as shown in (5a, 5b).

According to the divergence theorem, $\int \nabla \cdot \mathbf{V} dv = \oint \mathbf{V} \cdot \mathbf{n} dA$, we can calculate the divergence in the volume of $dv = \mathbf{g}_1 d\hat{x}^1 \times \mathbf{g}_2 d\hat{x}^2 \cdot \mathbf{g}_3 d\hat{x}^3 = J d\hat{x}^1 d\hat{x}^2 d\hat{x}^3$ in Figure 2. The flux of a velocity \mathbf{V} normal to the lower surface is $\mathbf{V} \cdot \mathbf{n} dA = \mathbf{V} \cdot (\mathbf{g}_1 d\hat{x}^1 \times \mathbf{g}_2 d\hat{x}^2) = \mathbf{V} \cdot \mathbf{g}_1 \times \mathbf{g}_2 d\hat{x}^1 d\hat{x}^2 = J \hat{v}^3 d\hat{x}^1 d\hat{x}^2 = J \hat{v}^3 d\hat{x}^1 d\hat{x}^2$, where $\hat{v}^3 = \mathbf{V} \cdot \mathbf{g}^3$, and the flux on the upper surfaces can be estimated by: $J \hat{v}^3 d\hat{x}^1 d\hat{x}^2 + \frac{\partial (J \hat{v}^3 d\hat{x}^1 d\hat{x}^2)}{\partial \hat{x}^3} d\hat{x}^3$. Hence, the net flux

along \mathbf{g}^3 is $\sim \frac{\partial (J \hat{v}^3)}{\partial \hat{x}^3} d\hat{x}^1 d\hat{x}^2 d\hat{x}^3$. It is also applied to two

other directions. The summation of the net fluxes becomes

$$\sum \mathbf{V} \cdot \mathbf{n} dA = \sum_{i=1}^3 \frac{\partial (J \hat{v}^i)}{\partial \hat{x}^i} d\hat{x}^1 d\hat{x}^2 d\hat{x}^3 \quad (8)$$

Therefore:

$$\begin{aligned} \int \nabla \cdot \mathbf{V} dv &= \sum \nabla \cdot \mathbf{V} (d\hat{x}^1 \mathbf{g}_1 \times d\hat{x}^2 \mathbf{g}_2 \cdot d\hat{x}^3 \mathbf{g}_3) \\ &= \sum \nabla \cdot \mathbf{V} (\mathbf{g}_1 \times \mathbf{g}_2 \cdot \mathbf{g}_3) d\hat{x}^1 d\hat{x}^2 d\hat{x}^3 = \sum \nabla \cdot \mathbf{V} J d\hat{x}^1 d\hat{x}^2 d\hat{x}^3 \\ &= \sum \mathbf{V} \cdot \mathbf{n} dA = \sum_{i=1}^3 \frac{\partial (J\hat{v}^i)}{\partial \hat{x}^i} d\hat{x}^1 d\hat{x}^2 d\hat{x}^3 \end{aligned}$$

and

$$\nabla \cdot \mathbf{V} = \frac{1}{J} \left(\frac{\partial (J\hat{v}^1)}{\partial \hat{x}^1} + \frac{\partial (J\hat{v}^2)}{\partial \hat{x}^2} + \frac{\partial (J\hat{v}^3)}{\partial \hat{x}^3} \right) \quad (9)$$

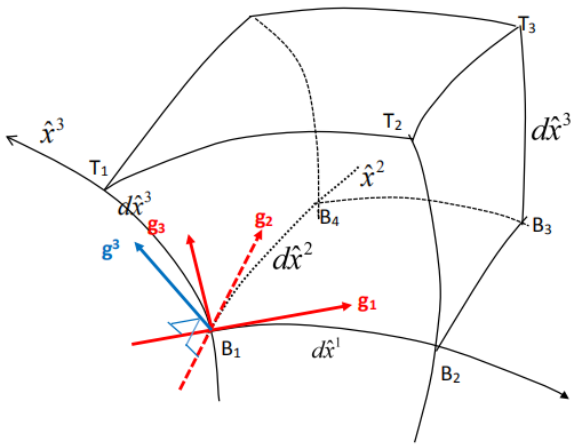


Figure 2. 3D curvilinear coordinates and volume

$$dv = (d\hat{x}^1 \mathbf{g}_1 \times d\hat{x}^2 \mathbf{g}_2 \cdot d\hat{x}^3 \mathbf{g}_3)$$

Following tensor analysis [19, 15], we can also derive divergence of a vector $\mathbf{V} = \hat{v}^j \mathbf{g}_j$:

$$\begin{aligned} \nabla \cdot \mathbf{V} &= \mathbf{g}^j \cdot \frac{\partial}{\partial \hat{x}^j} (\hat{v}^j \mathbf{g}_j) = \mathbf{g}^j \cdot \left(\frac{\partial \hat{v}^j}{\partial \hat{x}^j} \mathbf{g}_j + \hat{v}^j \frac{\partial \mathbf{g}_j}{\partial \hat{x}^j} \right) \\ &= \mathbf{g}^j \cdot \frac{\partial \hat{v}^j}{\partial \hat{x}^j} \mathbf{g}_j + \hat{v}^j \mathbf{g}^j \cdot \frac{\partial \mathbf{g}_j}{\partial \hat{x}^j} = \frac{\partial \hat{v}^j}{\partial \hat{x}^j} + \hat{v}^j \mathbf{g}^j \cdot \mathbf{g}_k \Gamma_{ji}^k \\ &= \frac{\partial \hat{v}^j}{\partial \hat{x}^j} + \hat{v}^j \Gamma_{ji}^j = \frac{\partial \hat{v}^j}{\partial \hat{x}^j} + \frac{\hat{v}^j}{J} \frac{\partial J}{\partial \hat{x}^j} = \frac{1}{J} \frac{\partial (J\hat{v}^j)}{\partial \hat{x}^j} \end{aligned} \quad (10)$$

where Christoffel of the second kind is defined as

$$\Gamma_{ij}^k = \Gamma_{ji}^k = g^{nk} \Gamma_{ijn} \quad (11a)$$

and

$$\Gamma_{ijk} = \mathbf{g}_k \cdot \frac{\partial \mathbf{g}_i}{\partial \hat{x}^j} = \frac{1}{2} \left(\frac{\partial g_{jk}}{\partial \hat{x}^i} + \frac{\partial g_{ik}}{\partial \hat{x}^j} - \frac{\partial g_{ij}}{\partial \hat{x}^k} \right) = \Gamma_{jik} \quad (11b)$$

is the Christoffel of the first kind, and

$$g_{ij} = \mathbf{g}_i \cdot \mathbf{g}_j; g^{k\ell} = \mathbf{g}^k \cdot \mathbf{g}^\ell; \text{ and } \frac{\partial \mathbf{g}_i}{\partial \hat{x}^j} = \Gamma_{ijk} \mathbf{g}^k = \Gamma_{ji}^k \mathbf{g}_k \quad (11c)$$

The curl of vector \mathbf{V} becomes

$$\begin{aligned} \nabla \times \mathbf{V} &= \mathbf{g}^1 \times \frac{\partial}{\partial \hat{x}^1} \mathbf{V} + \mathbf{g}^2 \times \frac{\partial}{\partial \hat{x}^2} \mathbf{V} + \mathbf{g}^3 \times \frac{\partial}{\partial \hat{x}^3} \mathbf{V} \\ &= J^{-1} \left((\mathbf{g}_2 \times \mathbf{g}_3) \times \frac{\partial}{\partial \hat{x}^1} \mathbf{V} + (\mathbf{g}_3 \times \mathbf{g}_1) \times \frac{\partial}{\partial \hat{x}^2} \mathbf{V} + (\mathbf{g}_1 \times \mathbf{g}_2) \times \frac{\partial}{\partial \hat{x}^3} \mathbf{V} \right) \\ &= J^{-1} \left(\mathbf{g}_3 \left(\mathbf{g}_2 \cdot \frac{\partial}{\partial \hat{x}^1} \mathbf{V} \right) + \mathbf{g}_1 \left(\mathbf{g}_3 \cdot \frac{\partial}{\partial \hat{x}^2} \mathbf{V} \right) + \mathbf{g}_2 \left(\mathbf{g}_1 \cdot \frac{\partial}{\partial \hat{x}^3} \mathbf{V} \right) \right) \\ &\quad - J^{-1} \left(\mathbf{g}_2 \left(\mathbf{g}_3 \cdot \frac{\partial}{\partial \hat{x}^1} \mathbf{V} \right) + \mathbf{g}_3 \left(\mathbf{g}_1 \cdot \frac{\partial}{\partial \hat{x}^2} \mathbf{V} \right) + \mathbf{g}_1 \left(\mathbf{g}_2 \cdot \frac{\partial}{\partial \hat{x}^3} \mathbf{V} \right) \right) \\ &= J^{-1} \left(\mathbf{g}_3 \frac{\partial}{\partial \hat{x}^1} (\mathbf{g}_2 \cdot \mathbf{V}) - \mathbf{g}_3 \frac{\partial \mathbf{g}_2}{\partial \hat{x}^1} \cdot \mathbf{V} - \mathbf{g}_2 \frac{\partial}{\partial \hat{x}^1} (\mathbf{g}_3 \cdot \mathbf{V}) + \mathbf{g}_2 \frac{\partial \mathbf{g}_3}{\partial \hat{x}^1} \cdot \mathbf{V} + \right. \\ &\quad \left. \mathbf{g}_1 \frac{\partial}{\partial \hat{x}^2} (\mathbf{g}_3 \cdot \mathbf{V}) - \mathbf{g}_1 \frac{\partial \mathbf{g}_3}{\partial \hat{x}^2} \cdot \mathbf{V} - \mathbf{g}_3 \frac{\partial}{\partial \hat{x}^2} (\mathbf{g}_1 \cdot \mathbf{V}) + \mathbf{g}_3 \frac{\partial \mathbf{g}_1}{\partial \hat{x}^2} \cdot \mathbf{V} + \right. \\ &\quad \left. \mathbf{g}_2 \frac{\partial}{\partial \hat{x}^3} (\mathbf{g}_1 \cdot \mathbf{V}) - \mathbf{g}_2 \frac{\partial \mathbf{g}_1}{\partial \hat{x}^3} \cdot \mathbf{V} - \mathbf{g}_1 \frac{\partial}{\partial \hat{x}^3} (\mathbf{g}_2 \cdot \mathbf{V}) + \mathbf{g}_1 \frac{\partial \mathbf{g}_2}{\partial \hat{x}^3} \cdot \mathbf{V} \right) \end{aligned} \quad (12a)$$

But

$$\frac{\partial \mathbf{g}_1}{\partial \hat{x}^2} = \frac{\partial}{\partial \hat{x}^2} \frac{\partial \mathbf{r}}{\partial \hat{x}^1} = \frac{\partial}{\partial \hat{x}^1} \frac{\partial \mathbf{r}}{\partial \hat{x}^2} = \frac{\partial \mathbf{g}_2}{\partial \hat{x}^1}$$

Therefore

$$\nabla \times \mathbf{V} = J^{-1} \begin{pmatrix} \mathbf{g}_3 \frac{\partial}{\partial \hat{x}^1} (\mathbf{g}_2 \cdot \mathbf{V}) - \mathbf{g}_2 \frac{\partial}{\partial \hat{x}^1} (\mathbf{g}_3 \cdot \mathbf{V}) + \\ \mathbf{g}_1 \frac{\partial}{\partial \hat{x}^2} (\mathbf{g}_3 \cdot \mathbf{V}) - \mathbf{g}_3 \frac{\partial}{\partial \hat{x}^2} (\mathbf{g}_1 \cdot \mathbf{V}) + \\ \mathbf{g}_2 \frac{\partial}{\partial \hat{x}^3} (\mathbf{g}_1 \cdot \mathbf{V}) - \mathbf{g}_1 \frac{\partial}{\partial \hat{x}^3} (\mathbf{g}_2 \cdot \mathbf{V}) \end{pmatrix}$$

Finally, we obtain:

$$\nabla \times \mathbf{V} = \frac{1}{J} \begin{bmatrix} \mathbf{g}_1 & \mathbf{g}_2 & \mathbf{g}_3 \\ \frac{\partial}{\partial \hat{x}^1} & \frac{\partial}{\partial \hat{x}^2} & \frac{\partial}{\partial \hat{x}^3} \end{bmatrix} \begin{bmatrix} \mathbf{g}_1 \cdot \mathbf{V} \\ \mathbf{g}_2 \cdot \mathbf{V} \\ \mathbf{g}_3 \cdot \mathbf{V} \end{bmatrix} = \frac{1}{J} \begin{bmatrix} \mathbf{g}_1 & \mathbf{g}_2 & \mathbf{g}_3 \\ \hat{v}_1 & \hat{v}_2 & \hat{v}_3 \end{bmatrix} \begin{bmatrix} \frac{\partial}{\partial \hat{x}^1} \\ \frac{\partial}{\partial \hat{x}^2} \\ \frac{\partial}{\partial \hat{x}^3} \end{bmatrix} \quad (12b)$$

where $\hat{v}_i = \mathbf{V} \cdot \mathbf{g}_i = \hat{v}^j \mathbf{g}^j \cdot \mathbf{g}_i$.

2.2 Terrain Following Coordinate

Terrain following coordinate is one of the most popular non-orthogonal systems applied to the atmospheric and oceanic models. Pielke [12] has detailed the history and evolution of the system. Figure 3 shows the 2D diagram

of the curvilinear coordinate (\hat{x}^1, \hat{x}^3) , the inclination angle θ of the \hat{z} -surface. For convenience, we also define the vertical coordinate $\hat{z} = \hat{x}^3$ and:

$$\hat{z} = \hat{x}^3 = \frac{z - z_b}{z_t - z_b} \tag{13}$$

where z_b is the terrain elevation and z_t is the domain height. From (13), we obtain:

$$\left(\frac{\partial \hat{z}}{\partial z}\right)_{x,y} = \frac{\partial \left(\frac{z - z_b}{z_t - z_b}\right)}{\partial z} = \frac{1}{(z_t - z_b)} \tag{14}$$

and

$$\begin{aligned} \left(\frac{\partial z}{\partial \hat{x}^3}\right)_{\hat{x}^1, \hat{x}^2} &= \left(\frac{\partial z}{\partial \hat{z}}\right)_{\hat{x}^1, \hat{x}^2} = \left(\frac{\partial (z_b + \hat{z}(z_t - z_b))}{\partial \hat{z}}\right)_{\hat{x}^1, \hat{x}^2} \\ &= (z_t - z_b) \end{aligned} \tag{15}$$

The inclinations of \hat{z} along x and y- directions are

$$\left(\frac{\partial z}{\partial x}\right)_{\hat{z}} = \left(\frac{\partial (z_b + \hat{z}(z_t - z_b))}{\partial x}\right)_{\hat{z}} = (1 - \hat{z}) \frac{\partial z_b}{\partial x} \tag{16a}$$

and

$$\left(\frac{\partial z}{\partial y}\right)_{\hat{z}} = (1 - \hat{z}) \frac{\partial z_b}{\partial y} \tag{16b}$$

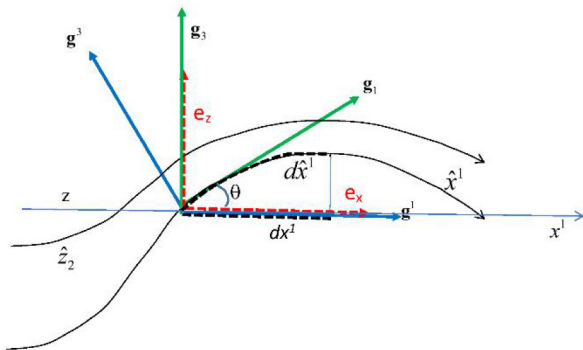


Figure 3. Basis vectors of 2D Cartesian coordinate and terrain following coordinates

The changes \hat{z} with respect to x and y are

$$\begin{aligned} \left(\frac{\partial \hat{z}}{\partial x}\right)_z &= \frac{\partial \left(\frac{z - z_b}{z_t - z_b}\right)}{\partial x} \\ &= \frac{(z_t - z_b) \frac{\partial (z - z_b)}{\partial x} - (z - z_b) \frac{\partial (z_t - z_b)}{\partial x}}{(z_t - z_b)^2} \\ &= \frac{\partial z_b}{\partial x} (\hat{z} - 1) \end{aligned} \tag{17a}$$

$$\left(\frac{\partial \hat{z}}{\partial y}\right)_z = \frac{\partial \left(\frac{z - z_b}{z_t - z_b}\right)}{\partial y} = \frac{\partial z_b}{\partial y} (\hat{z} - 1) \tag{17b}$$

The covariant basis vectors at the terrain coordinate system become:

$$\begin{aligned} \mathbf{g}_1 &= \left(\frac{\partial \mathbf{r}}{\partial \hat{x}^1}\right)_{\hat{x}^3} = \left(\frac{\partial (x\mathbf{e}_x + y\mathbf{e}_y + z\mathbf{e}_z)}{\partial \hat{x}^1}\right)_{\hat{x}^3} \\ &= \frac{\partial x}{\partial \hat{x}^1} \left[\mathbf{e}_x + \mathbf{e}_z (1 - \hat{z}) \frac{\partial z_b}{\partial x} \right] \end{aligned} \tag{18a}$$

$$\begin{aligned} \mathbf{g}_2 &= \left(\frac{\partial \mathbf{r}}{\partial \hat{x}^2}\right)_{\hat{x}^3} = \left(\frac{\partial (x\mathbf{e}_x + y\mathbf{e}_y + z\mathbf{e}_z)}{\partial \hat{x}^2}\right)_{\hat{x}^3} \\ &= \frac{\partial y}{\partial \hat{x}^2} \left[\mathbf{e}_y + \mathbf{e}_z (1 - \hat{z}) \frac{\partial z_b}{\partial y} \right] \end{aligned} \tag{18b}$$

and

$$\begin{aligned} \mathbf{g}_3 &= \left(\frac{\partial \mathbf{r}}{\partial \hat{x}^3}\right)_{\hat{x}^1, \hat{x}^2} = \left(\frac{\partial (x\mathbf{e}_x + y\mathbf{e}_y + z\mathbf{e}_z)}{\partial \hat{x}^3}\right)_{\hat{x}^1, \hat{x}^2} \\ &= (z_t - z_b) \mathbf{e}_z \end{aligned} \tag{18c}$$

At surface ($\hat{z} = 0$), \mathbf{g}_1 and \mathbf{g}_2 are parallel to the terrain surface, while \mathbf{g}_3 always points to the vertical direction. The Jacobian becomes

$$\begin{aligned}
 J = \mathbf{g}_1 \cdot \mathbf{g}_2 \times \mathbf{g}_3 &= \det \begin{bmatrix} \frac{\partial x}{\partial \hat{x}^1} & \frac{\partial x}{\partial \hat{x}^2} & \frac{\partial x}{\partial \hat{x}^3} \\ \frac{\partial y}{\partial \hat{x}^1} & \frac{\partial y}{\partial \hat{x}^2} & \frac{\partial y}{\partial \hat{x}^3} \\ \frac{\partial z}{\partial \hat{x}^1} & \frac{\partial z}{\partial \hat{x}^2} & \frac{\partial z}{\partial \hat{x}^3} \end{bmatrix} \\
 &= \det \begin{bmatrix} \frac{\partial x}{\partial \hat{x}^1} & 0 & 0 \\ 0 & \frac{\partial y}{\partial \hat{x}^2} & 0 \\ (1-\hat{z}) \frac{\partial z_b}{\partial x} \frac{\partial x}{\partial \hat{x}^1} & (1-\hat{z}) \frac{\partial z_b}{\partial y} \frac{\partial y}{\partial \hat{x}^2} & (z_t - z_b) \end{bmatrix} \\
 &= \frac{\partial x}{\partial \hat{x}^1} \frac{\partial y}{\partial \hat{x}^2} (z_t - z_b) \tag{19}
 \end{aligned}$$

From (2c), (5b) and (19), the contravariant basis vectors become

$$\begin{aligned}
 \mathbf{g}^1 &= \frac{\mathbf{g}_2 \times \mathbf{g}_3}{J} = \mathbf{e}_x \frac{\partial y}{\partial \hat{x}^2} (z_t - z_b) / \left(\frac{\partial x}{\partial \hat{x}^1} \frac{\partial y}{\partial \hat{x}^2} (z_t - z_b) \right) \\
 &= \mathbf{e}_x / \left(\frac{\partial x}{\partial \hat{x}^1} \right) = \left(\frac{\partial \hat{x}^1}{\partial x} \right) \mathbf{e}_j \tag{20a}
 \end{aligned}$$

$$\begin{aligned}
 \mathbf{g}^2 &= \frac{\mathbf{g}_3 \times \mathbf{g}_1}{J} = \mathbf{e}_y \frac{\partial x}{\partial \hat{x}^1} (z_t - z_b) / \left(\frac{\partial x}{\partial \hat{x}^1} \frac{\partial y}{\partial \hat{x}^2} (z_t - z_b) \right) \\
 &= \mathbf{e}_y / \frac{\partial y}{\partial \hat{x}^2} = \left(\frac{\partial \hat{x}^2}{\partial y} \right) \mathbf{e}_j \tag{20b}
 \end{aligned}$$

and

$$\begin{aligned}
 \mathbf{g}^3 &= \frac{\mathbf{g}_1 \times \mathbf{g}_2}{J} = \frac{\frac{\partial z_b}{\partial x} (\hat{z} - 1) \mathbf{e}_x}{(z_t - z_b)} + \frac{\frac{\partial z_b}{\partial y} (\hat{z} - 1) \mathbf{e}_y}{(z_t - z_b)} + \\
 &\frac{\mathbf{e}_z}{(z_t - z_b)} = \left(\frac{\partial \hat{x}^3}{\partial x^j} \right) \mathbf{e}_j \tag{20c}
 \end{aligned}$$

The transformation between the velocity (u, v, w) in the Cartesian coordinate (x, y, z) and the velocity ($\hat{u}, \hat{v}, \hat{w}$) in the new coordinate is

$$\begin{aligned}
 \begin{pmatrix} u \\ v \\ w \end{pmatrix} &= \begin{pmatrix} \frac{dx}{dt} \\ \frac{dy}{dt} \\ \frac{dz}{dt} \end{pmatrix} = \begin{pmatrix} \frac{\partial x}{\partial \hat{x}^1} \frac{d\hat{x}^1}{dt} + \frac{\partial x}{\partial \hat{x}^2} \frac{d\hat{x}^2}{dt} + \frac{\partial x}{\partial \hat{x}^3} \frac{d\hat{x}^3}{dt} \\ \frac{\partial y}{\partial \hat{x}^1} \frac{d\hat{x}^1}{dt} + \frac{\partial y}{\partial \hat{x}^2} \frac{d\hat{x}^2}{dt} + \frac{\partial y}{\partial \hat{x}^3} \frac{d\hat{x}^3}{dt} \\ \frac{\partial z}{\partial \hat{x}^1} \frac{d\hat{x}^1}{dt} + \frac{\partial z}{\partial \hat{x}^2} \frac{d\hat{x}^2}{dt} + \frac{\partial z}{\partial \hat{x}^3} \frac{d\hat{x}^3}{dt} \end{pmatrix} \\
 &= \begin{pmatrix} \frac{\partial x}{\partial \hat{x}^1} & 0 & 0 \\ 0 & \frac{\partial y}{\partial \hat{x}^2} & 0 \\ (1-\hat{z}) \frac{\partial z_b}{\partial x} \frac{\partial x}{\partial \hat{x}^1} & (1-\hat{z}) \frac{\partial z_b}{\partial y} \frac{\partial y}{\partial \hat{x}^2} & (z_t - z_b) \end{pmatrix} \begin{pmatrix} \hat{u}^1 \\ \hat{u}^2 \\ \hat{u}^3 \end{pmatrix} \\
 &= J \begin{pmatrix} \hat{u}^1 \\ \hat{u}^2 \\ \hat{u}^3 \end{pmatrix} \tag{21}
 \end{aligned}$$

and

$$\begin{aligned}
 \begin{pmatrix} \hat{u}^1 \\ \hat{u}^2 \\ \hat{u}^3 \end{pmatrix} &= \begin{pmatrix} \frac{d\hat{x}^1}{dt} \\ \frac{d\hat{x}^2}{dt} \\ \frac{d\hat{x}^3}{dt} \end{pmatrix} = \begin{pmatrix} \frac{\partial \hat{x}^1}{\partial x} & \frac{\partial \hat{x}^1}{\partial y} & \frac{\partial \hat{x}^1}{\partial z} \\ \frac{\partial \hat{x}^2}{\partial x} & \frac{\partial \hat{x}^2}{\partial y} & \frac{\partial \hat{x}^2}{\partial z} \\ \frac{\partial \hat{x}^3}{\partial x} & \frac{\partial \hat{x}^3}{\partial y} & \frac{\partial \hat{x}^3}{\partial z} \end{pmatrix} \begin{pmatrix} u \\ v \\ w \end{pmatrix} \\
 &= \begin{pmatrix} \frac{\partial \hat{x}^1}{\partial x} & 0 & 0 \\ 0 & \frac{\partial \hat{x}^2}{\partial y} & 0 \\ \frac{\frac{\partial z_b}{\partial x} (\hat{z} - 1)}{(z_t - z_b)} & \frac{\frac{\partial z_b}{\partial y} (\hat{z} - 1)}{(z_t - z_b)} & \frac{1}{(z_t - z_b)} \end{pmatrix} \begin{pmatrix} u \\ v \\ w \end{pmatrix} \\
 &= J^{-1} \begin{pmatrix} u \\ v \\ w \end{pmatrix} \tag{22}
 \end{aligned}$$

and

$$JJ^{-1} = \begin{pmatrix} \frac{\partial x}{\partial \hat{x}^1} & 0 & 0 \\ 0 & \frac{\partial y}{\partial \hat{x}^2} & 0 \\ (1-\hat{z}) \frac{\partial z_b}{\partial x} \frac{\partial x}{\partial \hat{x}^1} & (1-\hat{z}) \frac{\partial z_b}{\partial y} \frac{\partial y}{\partial \hat{x}^2} & (z_t - z_b) \end{pmatrix}$$

$$\begin{pmatrix} \frac{\partial \hat{x}^1}{\partial x} & 0 & 0 \\ 0 & \frac{\partial \hat{x}^2}{\partial y} & 0 \\ \frac{\partial z_b}{\partial x}(\hat{z}-1) & \frac{\partial z_b}{\partial x}(\hat{z}-1) & 1 \\ (z_t - z_b) & (z_t - z_b) & (z_t - z_b) \end{pmatrix} = \begin{pmatrix} 1 & 0 & 0 \\ 0 & 1 & 0 \\ 0 & 0 & 1 \end{pmatrix} = J^{-1}J \quad (23)$$

It shows that \mathbf{g}_3 parallels to \mathbf{e}_z , \mathbf{g}^1 parallels \mathbf{e}_x , and \mathbf{g}^2 parallels \mathbf{e}_y . In this system, \mathbf{g}_i is different from \mathbf{g}^i .

2.3 The Popular Terrain Following Coordinate

In the popular terrain coordinate ^[1, 5, 7, 12], it is assumed:

$$\bar{x} = x; \bar{y} = y; \text{ and } \bar{z} = \frac{z_t(z - z_b)}{z_t - z_b} \quad (24)$$

and the inverse transformation:

$$x = \bar{x}; y = \bar{y}; z = \frac{\bar{z}(z_t - z_b)}{z_t} + z_b \quad (25)$$

Because they assumed that $x = \bar{x}$ and $y = \bar{y}$, the spatial interval $\delta \bar{x}$ or $\delta \bar{y}$ is not measured along the real terrain as $\delta \hat{x}$ or $\delta \hat{y}$. The relationships of the basis vectors and other variables between the systems in 2.3 and 2.2 are:

$$\hat{z} = (z - z_b) / (z_t - z_b) = \bar{z} / z_t \quad (26a)$$

and

$$\frac{\partial x}{\partial \bar{x}^1} = 1 \text{ and } \frac{\partial y}{\partial \bar{x}^2} = 1, \text{ but } \frac{\partial x}{\partial \hat{x}^1} \text{ or } \frac{\partial y}{\partial \hat{x}^2} \text{ can be different from 1.} \quad (26b)$$

Their basic vector $\bar{\mathbf{g}}_i$ and the relationship with \mathbf{g}_i are;

$$\begin{aligned} \bar{\mathbf{g}}_1 &= \frac{\partial \mathbf{r}}{\partial \bar{x}^1} = \left(\frac{\partial (x\mathbf{e}_x + y\mathbf{e}_y + z\mathbf{e}_z)}{\partial \bar{x}^1} \right)_{\bar{x}^3} \\ &= \left(\frac{\partial x}{\partial \bar{x}^1} \mathbf{e}_x + \mathbf{e}_z \frac{\partial}{\partial \bar{x}^1} \left(\frac{\bar{z}(z_t - z_b)}{z_t} + z_b \right) \right)_{\bar{x}^3} \\ &= \left(\frac{\partial x}{\partial \bar{x}^1} \mathbf{e}_x + \mathbf{e}_z \frac{\partial z_b}{\partial \bar{x}^1} (1 - \frac{\bar{z}}{z_t}) \right)_{\bar{x}^3} = \frac{\partial x}{\partial \bar{x}^1} \left(\mathbf{e}_x + \mathbf{e}_z (1 - \hat{z}) \frac{\partial z_b}{\partial x} \right)_{\bar{x}^3} \\ &= \frac{\partial \hat{x}^1}{\partial \bar{x}^1} \mathbf{g}_1 \end{aligned} \quad (27a)$$

$$\bar{\mathbf{g}}_2 = \frac{\partial \mathbf{r}}{\partial \bar{x}^2} = \left(\frac{\partial (x\mathbf{e}_x + y\mathbf{e}_y + z\mathbf{e}_z)}{\partial \bar{x}^2} \right)_{\bar{x}^3}$$

$$\begin{aligned} &= \frac{\partial y}{\partial \bar{x}^2} \left[\mathbf{e}_y + \mathbf{e}_z \frac{(z_t - \bar{z})}{z_t} \frac{\partial z_b}{\partial y} \right] \\ &= \frac{\partial y}{\partial \bar{x}^2} \left(\mathbf{e}_y + \mathbf{e}_z (1 - \hat{z}) \frac{\partial z_b}{\partial y} \right) = \frac{\partial \mathbf{r}}{\partial \bar{x}^2} = \frac{\partial \hat{x}^2}{\partial \bar{x}^2} \mathbf{g}_2 \end{aligned} \quad (27b)$$

$$\begin{aligned} \bar{\mathbf{g}}_3 &= \left(\frac{\partial \mathbf{r}}{\partial \bar{x}^3} \right)_{\bar{x}^1, \bar{x}^2} = \left(\frac{\partial (x\mathbf{e}_x + y\mathbf{e}_y + z\mathbf{e}_z)}{\partial \bar{x}^3} \right)_{\bar{x}^1, \bar{x}^2} \\ &= \mathbf{e}_z \frac{(z_t - z_b)}{z_t} = \frac{\partial \mathbf{r}}{\partial \bar{x}^3} = \frac{\mathbf{g}_3}{z_t} \end{aligned} \quad (27c)$$

and the Jacobian

$$\begin{aligned} \bar{J} &= \bar{\mathbf{g}}_1 \cdot \bar{\mathbf{g}}_2 \times \bar{\mathbf{g}}_3 = \det \begin{bmatrix} \frac{\partial \mathbf{r}}{\partial \bar{x}^1} & \dots & \frac{\partial \mathbf{r}}{\partial \bar{x}^3} \end{bmatrix} = \det \begin{bmatrix} \frac{\partial x}{\partial \bar{x}^1} & \frac{\partial x}{\partial \bar{x}^2} & \frac{\partial x}{\partial \bar{x}^3} \\ \frac{\partial y}{\partial \bar{x}^1} & \frac{\partial y}{\partial \bar{x}^2} & \frac{\partial y}{\partial \bar{x}^3} \\ \frac{\partial z}{\partial \bar{x}^1} & \frac{\partial z}{\partial \bar{x}^2} & \frac{\partial z}{\partial \bar{x}^3} \end{bmatrix} \\ &= \det \begin{bmatrix} \frac{\partial x}{\partial \bar{x}^1} & 0 & 0 \\ 0 & \frac{\partial y}{\partial \bar{x}^2} & 0 \\ \frac{\partial z_b}{\partial \bar{x}^1} \frac{(z_t - \bar{z})}{z_t} & \frac{\partial z_b}{\partial \bar{x}^2} \frac{(z_t - \bar{z})}{z_t} & \frac{(z_t - z_b)}{z_t} \end{bmatrix} = \frac{(z_t - z_b)}{z_t} \end{aligned} \quad (28)$$

as well as

$$\bar{\mathbf{g}}^1 = \bar{\mathbf{g}}_2 \times \bar{\mathbf{g}}_3 / \bar{J} = \frac{(z_t - z_b)}{z_t} \mathbf{e}_y \times \frac{z_t \mathbf{e}_z}{(z_t - z_b)} = \mathbf{e}_x = \mathbf{g}^1 \frac{\partial \hat{x}^1}{\partial x} \quad (29a)$$

$$\bar{\mathbf{g}}^2 = \bar{\mathbf{g}}_3 \times \bar{\mathbf{g}}_1 / \bar{J} = \mathbf{e}_y = \mathbf{g}^2 \frac{\partial \hat{x}^2}{\partial y} \quad (29b)$$

$$\begin{aligned} \bar{\mathbf{g}}^3 &= \bar{\mathbf{g}}_1 \times \bar{\mathbf{g}}_2 / \bar{J} \\ &= \left(\frac{\partial x}{\partial \bar{x}^1} \mathbf{e}_x + \mathbf{e}_z \frac{\partial z_b}{\partial \bar{x}^1} (1 - \frac{\bar{z}}{z_t}) \right)_{\bar{x}^3} \\ &= \left[\frac{\partial y}{\partial \bar{x}^2} \mathbf{e}_y + \mathbf{e}_z \frac{(z_t - \bar{z})}{z_t} \frac{\partial z_b}{\partial \bar{x}^2} \right] / \frac{(z_t - z_b)}{z_t} \\ &= \frac{z_t}{(z_t - z_b)} \mathbf{e}_z - \frac{(z_t - \bar{z})}{(z_t - z_b)} \frac{\partial z_b}{\partial y} \mathbf{e}_y - \frac{(z_t - \bar{z})}{(z_t - z_b)} \frac{\partial z_b}{\partial x} \mathbf{e}_x \\ &= z_t \left[\frac{(\hat{z}-1)}{(z_t - z_b)} \frac{\partial z_b}{\partial x} \mathbf{e}_x + \frac{(\hat{z}-1)}{(z_t - z_b)} \frac{\partial z_b}{\partial y} \mathbf{e}_y + \frac{1}{(z_t - z_b)} \mathbf{e}_z \right] \\ &= z_t \mathbf{g}^3 \end{aligned} \quad (29c)$$

The velocity becomes

$$\begin{pmatrix} \bar{u} \\ \bar{v} \\ \bar{w} \end{pmatrix} = \begin{pmatrix} \frac{d\bar{x}^1}{dt} \\ \frac{d\bar{x}^2}{dt} \\ \frac{d\bar{x}^3}{dt} \end{pmatrix} = \begin{pmatrix} \frac{\partial \bar{x}^1}{\partial x} & \frac{\partial \bar{x}^1}{\partial y} & \frac{\partial \bar{x}^1}{\partial z} \\ \frac{\partial \bar{x}^2}{\partial x} & \frac{\partial \bar{x}^2}{\partial y} & \frac{\partial \bar{x}^2}{\partial z} \\ \frac{(\bar{z}-z_t)\partial z_b/\partial x}{(z_t-z_b)} & \frac{(\bar{z}-z_t)\partial z_b/\partial y}{(z_t-z_b)} & \frac{z_t}{(z_t-z_b)} \end{pmatrix} \begin{pmatrix} u \\ v \\ w \end{pmatrix} = \begin{pmatrix} 1 & 0 & 0 \\ 0 & 1 & 0 \\ \frac{(\bar{z}-z_t)\partial z_b/\partial x}{(z_t-z_b)} & \frac{(\bar{z}-z_t)\partial z_b/\partial y}{(z_t-z_b)} & \frac{z_t}{(z_t-z_b)} \end{pmatrix} \begin{pmatrix} u \\ v \\ w \end{pmatrix} \quad (30)$$

Eq. (30) was derived by Gal-Chen and Somerville^[1]. It is noted that

$$\bar{u} = \frac{d\bar{x}^1}{dt} = \frac{dx}{dt} = u = \hat{u} \frac{\partial x}{\partial \bar{x}^1}, \quad (31a)$$

$$\bar{v} = \frac{d\bar{x}^2}{dt} = \frac{dy}{dt} = v = \hat{v} \frac{\partial y}{\partial \bar{x}^2}, \quad (31b)$$

Hence, their system becomes very simple, and

$$\begin{aligned} \bar{w} &= \frac{d\bar{x}^3}{dt} = \left(\frac{(\bar{z}-z_t)\partial z_b/\partial x}{(z_t-z_b)} u + \frac{(\bar{z}-z_t)\partial z_b/\partial y}{(z_t-z_b)} v + \frac{z_t}{(z_t-z_b)} w \right) \\ &= z_t \frac{d\hat{z}}{dt} = z_t \left(-\frac{(1-\hat{z})\partial z_b/\partial x}{(z_t-z_b)} u - \frac{(1-\hat{z})\partial z_b/\partial y}{(z_t-z_b)} v + \frac{1}{(z_t-z_b)} w \right) \\ &= z_t \hat{u}^3 \end{aligned} \quad (31c)$$

The corresponding gradient, the divergence, and curl are

$$\nabla S = \bar{\mathbf{g}}^i \frac{\partial S}{\partial \bar{x}^i}, \quad (32)$$

$$\nabla \cdot \mathbf{V} = \frac{1}{J} \left(\frac{\partial(\bar{J}\bar{v}^1)}{\partial \bar{x}^1} + \frac{\partial(\bar{J}\bar{v}^2)}{\partial \bar{x}^2} + \frac{\partial(\bar{J}\bar{v}^3)}{\partial \bar{x}^3} \right), \quad (33)$$

and

$$\nabla \times \mathbf{V} = \frac{1}{J} \begin{bmatrix} \bar{\mathbf{g}}_1 & \bar{\mathbf{g}}_2 & \bar{\mathbf{g}}_3 \\ \frac{\partial}{\partial \bar{x}^1} & \frac{\partial}{\partial \bar{x}^2} & \frac{\partial}{\partial \bar{x}^3} \\ \bar{\mathbf{g}}_1 \cdot \mathbf{V} & \bar{\mathbf{g}}_2 \cdot \mathbf{V} & \bar{\mathbf{g}}_3 \cdot \mathbf{V} \end{bmatrix}$$

$$= \frac{1}{J} \begin{bmatrix} \bar{\mathbf{g}}_1 & \bar{\mathbf{g}}_2 & \bar{\mathbf{g}}_3 \\ \frac{\partial}{\partial \bar{x}^1} & \frac{\partial}{\partial \bar{x}^2} & \frac{\partial}{\partial \bar{x}^3} \\ \bar{v}_1 & \bar{v}_2 & \bar{v}_3 \end{bmatrix}. \quad (34)$$

3. Numerical Simulations

We apply a 2D numerical model to test the curvilinear coordinates on gradient, divergence, and curl, which are the fundamental operators in the Navier-Stokes equations. The 2D model consists of 2 sets of grids: The first one is the C-grids in the Cartesian coordinate without mountain. The second set is derived from the coordinates discussed in Sections 2.2-2.3. The numerical results derived from the Cartesian coordinate are used to compare with the simulations obtained from the curvilinear systems. The Cartesian 2D model includes (20×20) uniform grids with Δx=1 km, z_t = 12 km, and Δz = 12 km/20. The elevation of a bell-shaped mountain is given by

$$z_b = z_{bm} / \left(\left(\frac{x-x_c}{wa} \right)^2 + 1.0 \right) \quad (35)$$

where z_{bm} = 2000 m, wa = 4000 m, and x_c is located at the mid-point in the x-axis. The coordinate \hat{z} is given by (13) and \bar{z} by (24).

3.1 Gradient

$$\text{A scalar variable, } S = Cs(x-x_c)z, \quad (36a)$$

with Cs=3.0. The second order centered difference of the gradient in the Cartesian coordinate is:

$$\nabla S = \frac{\partial S}{\partial x} \mathbf{e}_x + \frac{\partial S}{\partial z} \mathbf{e}_z = \frac{S_{j+1/2,k} - S_{j-1/2,k}}{\Delta x} \mathbf{e}_x + \frac{S_{j,k+1/2} - S_{j,k-1/2}}{\Delta z} \mathbf{e}_z \quad (36b)$$

The numerical scheme in the terrain following coordinate in Sect. 2.2 is:

$$\begin{aligned} \nabla S &= \mathbf{g}^j \frac{\partial S}{\partial \hat{x}^j} = \frac{\mathbf{e}_x}{\partial x / \partial \hat{x}^1} \frac{\partial S}{\partial \hat{x}^1} + \left(\frac{\partial z_b}{\partial x} (\hat{z}-1) \mathbf{e}_x + \frac{\mathbf{e}_z}{(z_t-z_b)} \right) \frac{\partial S}{\partial \hat{x}^3} \\ &= \left(\frac{1}{\partial x / \partial \hat{x}^1} \frac{\partial S}{\partial \hat{x}^1} + \frac{\partial z_b}{\partial x} (\hat{z}-1) \frac{\partial S}{\partial \hat{x}^3} \right) \mathbf{e}_x + \left(\frac{1}{(z_t-z_b)} \right) \frac{\partial S}{\partial \hat{x}^3} \mathbf{e}_z \end{aligned} \quad (36c)$$

The scheme in Sect. 2.3 is

$$\begin{aligned} \nabla S &= \bar{\mathbf{g}}^j \frac{\partial S}{\partial \bar{x}^j} \\ &= \frac{\mathbf{e}_x}{\partial x / \partial \bar{x}^1} \frac{\partial S}{\partial \bar{x}^1} + \left(\frac{(\bar{z} - z_t)}{(z_t - z_b)} \frac{\partial z_b}{\partial x} \mathbf{e}_x + \frac{z_t}{(z_t - z_b)} \mathbf{e}_z \right) \frac{\partial S}{\partial \bar{x}^3} \\ &= \left(\frac{1}{\partial x / \partial \bar{x}^1} \frac{\partial S}{\partial \bar{x}^1} + \frac{(\bar{z} - z_t)}{(z_t - z_b)} \frac{\partial z_b}{\partial x} \frac{\partial S}{\partial \bar{x}^3} \right) \mathbf{e}_x + \frac{z_t}{(z_t - z_b)} \frac{\partial S}{\partial \bar{x}^3} \mathbf{e}_z \end{aligned} \quad (36d)$$

The continuous black lines in Figure 4 show the gradient in the Cartesian coordinate of Eq. (36b) along \mathbf{e}_x and \mathbf{e}_z directions, respectively. They are completely covered by the dashed red lines from the terrain following coordinates of Eq. (36c) and the blue dots of Eq. (36d). We can see that both schemes generate the same results as the Cartesian coordinate, because

$$\begin{aligned} \left(\mathbf{e}_x / \frac{\partial x}{\partial \bar{x}^1} \right) \left(\frac{\partial S}{\partial x} \frac{\partial x}{\partial \bar{x}^1} + \frac{\partial S}{\partial z} \frac{\partial z}{\partial \bar{x}^1} \right) &= \\ \left(\mathbf{e}_x / \frac{\partial x}{\partial \bar{x}^1} \right) \left(\frac{\partial S}{\partial x} \frac{\partial x}{\partial \bar{x}^1} + \frac{\partial S}{\partial z} \frac{\partial z}{\partial \bar{x}^1} \right) &= \mathbf{e}_x \left(\frac{\partial S}{\partial x} + \frac{\partial S}{\partial z} \frac{\partial z}{\partial x} \right). \end{aligned}$$

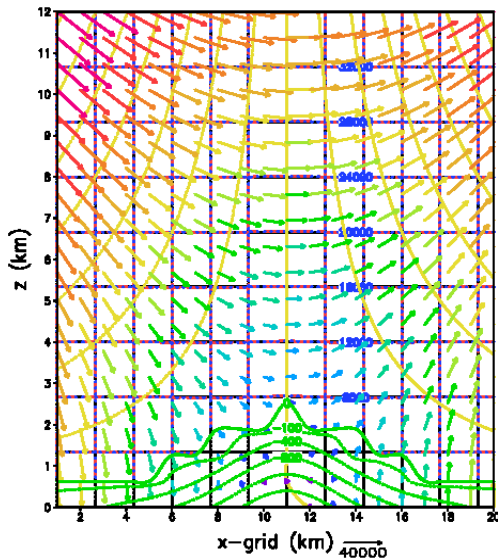


Figure 4. S in (36a) is shown by yellow lines, ∇S by color vector; x and z components of gradient in Cartesian coordinate by black lines, which are covered by dashed red lines of (36c) and blue dots of (36d) in terrain following coordinates. Green lines show terrain and depth beneath (in meter.)

3.2 Divergence

$$\mathbf{V} = Dc(x - x_c)z^2 \mathbf{e}_x + Dc(x - x_c)^2 z \mathbf{e}_z \quad (37a)$$

with $Dc = 6 \times 10^{-8}$, is applied to the Cartesian and terrain following coordinates. Then we solve the divergences numerically:

$$Div_a = \nabla \cdot \mathbf{V} = \frac{\partial v}{\partial x} + \frac{\partial w}{\partial z}, \quad (37b)$$

$$Div_b = \nabla \cdot \mathbf{V} = \mathbf{g}^j \frac{\partial}{\partial \hat{x}^j} \cdot (\hat{v}^i \mathbf{g}_i) = \frac{1}{J} \frac{\partial}{\partial \hat{x}^j} (J \hat{v}^j) \quad (37c)$$

and

$$Div_c = \nabla \cdot \mathbf{V} = \bar{\mathbf{g}}^j \frac{\partial}{\partial \bar{x}^j} \cdot (\bar{v}^i \bar{\mathbf{g}}_i) = \frac{1}{\bar{J}} \frac{\partial}{\partial \bar{x}^j} (\bar{J} \bar{v}^j) \quad (37d)$$

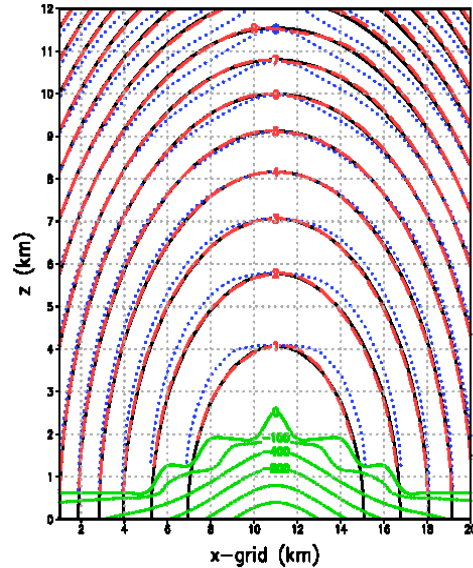


Figure 5. Black lines for divergence from (37b) in Cartesian, dashed red lines from (37c), and blue dots from (37d) of terrain following coordinates

Figure 5 shows Div_a of the Cartesian coordinate (black lines), as well as Div_b (dashed red lines) and Div_c (blue dots) from the terrain following coordinates. Div_b agrees with Div_a . But Div_c departs from Div_a over the slope of the mountain, especially in the lower layers, where the difference between $\delta \bar{x}^1$ and $\delta \hat{x}^1$ is large. The discrepancy diminishes when $\delta \bar{x}^1$ approaches $\delta \hat{x}^1$ in the upper layer or over the peak of the mountain (at $x = x_c$). Hence, the difference between $d\bar{x}^1$ and $d\hat{x}^1$ is important.

3.3 Curl along y-direction

The vector \mathbf{V} is given by

$$\mathbf{V} = 2.526 \times 10^6 (x - x_c) z \mathbf{e}_x + 2.526 \times 10^3 (x - x_c) (z - 10\Delta z)^2 \mathbf{e}_z \quad (38a)$$

The y-component of curls becomes

$$Curl_a = \frac{\partial u}{\partial z} - \frac{\partial w}{\partial x}, \quad (38b)$$

$$Curl_b = \frac{1}{J} \left(\frac{\partial \hat{v}_1}{\partial \hat{x}^3} - \frac{\partial \hat{v}_3}{\partial \hat{x}^1} \right), \quad (38c)$$

And

$$Curl_c = \frac{1}{\bar{J}} \left(\frac{\partial \bar{v}_1}{\partial \bar{x}^3} - \frac{\partial \bar{v}_3}{\partial \bar{x}^1} \right). \quad (38d)$$

The results of $Curl_a$ (black), $Curl_b$ (dashed red), and $Curl_c$ (blue dots) are shown in Figure 6. Overall, $Curl_b$ reproduces $Curl_a$ quite well, except some errors in the short-waves, because the solutions obtained from terrain following coordinates are interpreted to the Cartesian grids by linear interpretation. But $Curl_c$ can be quite different from $Curl_a$, as discussed in Section 3.2.

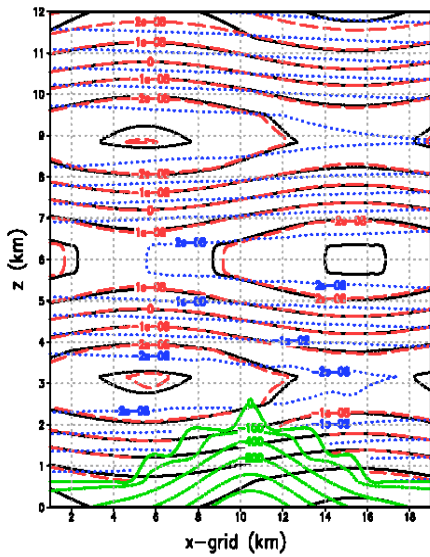


Figure 6. y-component curl: Black lines from (38b) of Cartesian coordinate, dashed red lines from (38c) and blue dots from (38d) of terrain following coordinates, and green lines for terrain

4. The Navier-Stokes Equations

The equations in geofluid dynamics in the Cartesian system are:

$$\frac{\partial \rho}{\partial t} + \frac{\partial(\rho u_j)}{\partial x_j} = 0 \quad (39)$$

$$\frac{\partial u_i}{\partial t} + u_j \frac{\partial u_i}{\partial x_j} = -\frac{1}{\rho} \frac{\partial p}{\partial x_j} + b_i + F_{ri} = \frac{F_i}{\rho} \quad (40)$$

$$\frac{\partial \theta}{\partial t} + u_j \frac{\partial \theta}{\partial x_j} = \frac{1}{c_p} \frac{\theta}{T} \frac{dq}{dt} + D_\theta \quad (41)$$

and equation of state

$$f(p, \rho, T) = 0 \quad (42)$$

where p is pressure, ρ is density, b_i is gravity, F_{ri} is friction along the x_i -direction, θ is potential temperature, T is temperature, q is heating, and D_θ is diffusion. Applying the chain rule to the pressure gradient, divergence, and the total derivatives in the curvilinear coordinate^[21], we obtain:

$$\frac{\partial \rho}{\partial t} + \left(\frac{\partial(\rho u_j)}{\partial x_j} \Big|_{\hat{x}_3} - \frac{\partial(\rho u_j)}{\partial z} \frac{\partial z}{\partial x_j} \Big|_{\hat{x}_3} \right) + \frac{\partial(\rho u_3)}{\partial \hat{x}_3} = 0 \quad (43)$$

for $j=1$ and 2

$$\frac{\partial u_i}{\partial t} + \hat{u}^j \frac{\partial u_i}{\partial \hat{x}_j} = -\frac{1}{\rho} \left(\frac{\partial p}{\partial x_i} \Big|_{\hat{x}_3} - \frac{\partial p}{\partial z} \frac{\partial z}{\partial x_i} \Big|_{\hat{x}_3} \right) + b_i + \frac{F_{ri}}{\rho} \quad (44)$$

and

$$\frac{\partial \theta}{\partial t} + \hat{u}^j \frac{\partial \theta}{\partial \hat{x}_j} = \frac{1}{c_p} \frac{\theta}{T} \frac{dq}{dt} + D_\theta \quad (45)$$

Eqs. (43-45) have been applied to the NTU-Purdue Nonhydrostatic model^[20], and other nonhydrostatic models^[21,22]. Although the system is simple and can be solved numerically with high accuracy^[10,23,24], it does not conserve the total mass or momentum. Combining those equations, we obtain the flux forms:

$$\frac{\partial u_i \rho}{\partial t} + \frac{\partial(u_i \rho u_j)}{\partial x_j} = -\frac{\partial p}{\partial x_j} + b_i + F_{ri} = F_i \quad (46)$$

and

$$\frac{\partial \rho \theta}{\partial t} + \frac{\partial \rho \theta u_j}{\partial x_j} = \frac{1}{c_p} \frac{\theta \rho}{T} \frac{dq}{dt} + D_\theta \rho = Q \quad (47)$$

Without forcing terms on the right-hand side, Eq. (40) in the curvilinear coordinate becomes

$$\frac{\partial \hat{v}^j \mathbf{g}_j}{\partial t} = -\hat{v}^i \mathbf{g}_i \cdot \mathbf{g}^i \frac{\partial}{\partial \hat{x}^i} (\hat{v}^j \mathbf{g}_j), \quad (48)$$

or

$$\frac{\partial \hat{v}^k}{\partial t} = -\hat{v}^i \frac{\partial \hat{v}^k}{\partial \hat{x}^i} - \hat{v}^i \hat{v}^j \frac{\partial \mathbf{g}_j}{\partial \hat{x}^i} \cdot \mathbf{g}^k.$$

With terrain given by (35), and the velocity:

$\mathbf{v} = 4\sin(\pi x/x_L)\sin(2\pi z/z_L)\mathbf{e}_x + \sin(2\pi x/x_L)\sin(\pi z/z_L)\mathbf{e}_z$, where $x_L=20 \Delta x$, is the length of horizontal domain, z_L is the height of the domain, we calculate the local change of velocities $(\hat{u}, \hat{v}, \hat{w})$ and $(\bar{u}, \bar{v}, \bar{w})$ in the terrain following coordinates. Then, they are converted to the Cartesian coordinate according to (21) and (31) to compare with (u, v, w) calculated from the Cartesian coordinate. The numerical results of time-derivative of x-component velocities in Figure 7 show that $(\hat{x}^1, \hat{x}^2, \hat{x}^3)$ is better than $(\bar{x}^1, \bar{x}^2, \bar{x}^3)$ as expected.

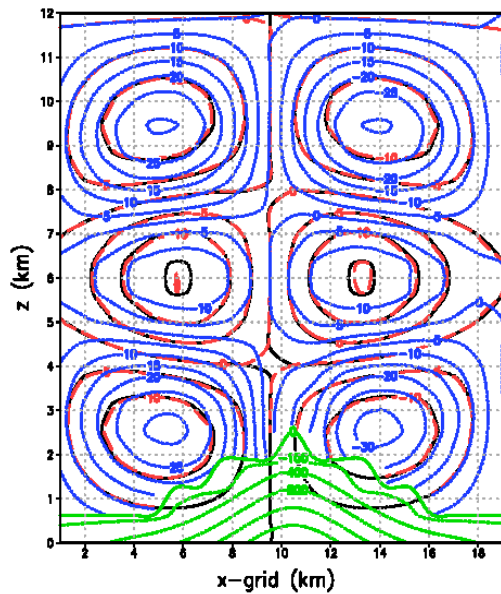


Figure 7. Local time derivative of u: black lines from Cartesian coordinate, red from (48) based on $(\hat{x}, \hat{y}, \hat{z})$ coordinate, and blue dots based on $(\bar{x}, \bar{y}, \bar{z})$ coordinate

The conventional flux form of momentum in the curvilinear is

$$\frac{\partial \rho \hat{v}^j}{\partial t} + \frac{1}{J} \frac{\partial}{\partial \hat{x}^i} (J \rho \hat{v}^i \hat{v}^j) - \mathbf{g}_k \hat{v}^i \hat{v}^k \cdot \frac{\partial \mathbf{g}^j}{\partial \hat{x}^i} = -\mathbf{g}^j \cdot \mathbf{g}^i \frac{\partial p}{\partial \hat{x}^i} + \dots \quad (49)$$

In the Cartesian coordinate, the component momentum over the entire domain $(\sum u_i \rho dv)$ in (46) is conserved with $F_i = 0$. $\sum \rho \theta dv$ in (47) is also conserved if $Q = 0$. But (49) is not conserved with $F_i = 0$ [17], it is also quite complicated. In the curvilinear systems, we may use the divergence operator to present the flux form of the equations, i.e.,

$$\frac{\partial \psi}{\partial t} = -\nabla \cdot (\psi \mathbf{v}) = -\frac{1}{J} \frac{\partial}{\partial \hat{x}^j} (J \psi \hat{v}^j) = -\frac{1}{J} \frac{\partial}{\partial \hat{x}^j} (J \tilde{v}^j) \quad (50)$$

where $\tilde{v}^j = \psi \hat{v}^j$, $\psi = \rho$ in (39), $\psi = \rho \theta$ in (47), and $\psi = \rho u_i$ in (46) where u_i is the i-component velocity in the Cartesian coordinate. Eq. (50) is much simpler than (49) and can be solved easily. Eq. (48) and (49) can also be written:

$$\frac{\partial(\rho J)}{\partial t} = -\frac{\partial(\rho J \hat{u}^i)}{\partial \hat{x}^i} \quad (51)$$

and

$$\frac{\partial(\rho J u_j)}{\partial t} = -\frac{\partial(\rho J \hat{u}^i u_j)}{\partial \hat{x}^i} + F_j \quad (52)$$

The total mass is conserved in (51), and total momentum along each component (u_j in Cartesian coordinate) is also conserved with $F_j = 0$ in (52). They can be calculated as divergence operator in the previous section. The Navier-Stokes equations including forcing terms can be solved by the finite volume method [25].

5. Summary

Here we provide the derivations of a terrain following coordinate, in which the gradient is calculated along the coordinate curves, $\frac{\partial \psi}{\partial \hat{x}^j}$, with a variable spatial interval

$\delta \hat{x}^j$. The results obtained from the gradient, divergence and curl are consistent with those derived from the Cartesian grids. On the other hand, the system proposed by Gal-Chen and Somerville and others with $\delta \bar{x}^j = \delta x^j$ along the horizontal coordinate, introduces significant errors in divergence and curl over the sloped terrain.

When the proposed terrain following coordinate is applied to the Navier-Stokes equations, the results agree with those calculated from the Cartesian coordinate. On the other hand, discrepancy shows in the popular terrain following coordinate. Meanwhile the total mass, momentum, and energy become conserved by using a modified flux form of (51-52). It is also noted that the chain rule proposed by Kasahara works well for gradient, divergence, and curl operators, but they do not conserve the total mass, momentum, or energy when they are applied to the Navier-Stokes equations.

Acknowledgments

The author thanks Prof. K. Tsuboki at Nagoya University for useful discussions, and Prof. P. Lim and National Central University for providing helps and the computing facility.

References

- [1] Gar-Chen, T., R. C. J. Somerville. Numerical solution of the Navier-Stokes equations with topography. *J. Comput. Phys.*, 1975, 17: 276-309.
- [2] Kasahara, A.. Various Vertical Coordinate Systems Used for Numerical Weather Prediction., *Mon. Wea. Rev.*, 1974, 102(7): 509- 522.
- [3] Sun, W. Y., J. D. Chern. Diurnal variation of lee-vortexes in Taiwan and surrounding area. *J. Atmos. Sci.*, 1993, 50: 3404-3430.
- [4] Pacanowski, R. C. MOM 2 Documentation User's Guide and Reference Manual version 1.0. GFDL Ocean Technical Report #3. 233pp. GFDL, NOAA, 1995.
- [5] Saito K, K. T. Kato, H. Eito, C. Muroi. Documentation of the Meteorological Research Institute/Numerical Prediction Division Unified Nonhydrostatic Model. MRI Report, 2001, 42: 133.
- [6] Staniforth A., W. White, N. Wood, J. Thuburn, M. Zerroukat, E. Corderro. Unified Model Documentation Paper. Joy of U.M. 6.0- Model Formulation. Dynamics Research Numerical Weather Prediction. Met Office, Devan, United Kingdom, 2004, 15.
- [7] Tsuboki K., A. Sakakibara. Numerical Prediction of High-Impact Weather Systems, HYARC, Nagoya, 2007: 273.
- [8] Skamarock, W. C., J. B. Klemp, J. Dudhia, D. O. Gill, D. M. Barker, M. G. Duda, X.-Y. Huang, W. Wang, J. G. Powers. A Description of Advanced Research WRF Version 3. NCAR/TN- 475+STR, 2008: 113pp
- [9] Lin, M-Y, W. Y. Sun, M-D. Chiou, C-Y. Chen, H.-Y. Cheng, C.-H. Chen:. Development and evaluation of a storm surge warning system in Taiwan. *Ocean Dynamics*, 2018.
DOI: <https://doi.org/10.1007/s10236-018-1179-z>
- [10] Sun, W.Y., O. M. Sun. Revisiting the parcel method and CAPE, *Dynamics of Atmospheres and Oceans*, , 2019, 86: 134-152.
- [11] Kapitza, H., D. P. Eppel. The non-hydrostatic mesoscale GESIMA. Part I: Dynamical equations and tests. *Beitr. Phys. Atmosph.*, 1992, 65: 129-145.
- [12] Pielke, Sr R. A. Mesoscale Meteorological Modeling. 2nd Ed. Academic Press, USA, 2002: 676.
- [13] Pielke, R. A., W. R. cotton, R. L. Walko, C. J. Tremback, W. A. Lyons, L. D. Grasso, M. E. Nicholls, M. D. Moran, D. A. Wesley, T. J. Lee, J. H. Copeland. A comprehensive meteorological modeling system-RAMS. *Meteor. Atmos. Phys.*, 1992, 49: 69-91.
- [14] Sun, W. Y, O. M. Sun, K. Tsuboki. A Modified Atmospheric Nonhydrostatic Model on Low Aspect Ratio Grids-Part II. *Tellus A* 2013, 65: 19681
DOI: <http://dx.doi.org/10.3402/tellusa.v65i0.19681>
- [15] Kusse, B. R., E. Westwig. *Mathematical Physics*, 2nd Ed. Wiley-VCH, Weinheim, Germany, 2006: 699.
- [16] Kajishima, T., K. Taira. *Computational Fluid Dynamics*, Springer. Switzerland, , 2017: 358.
- [17] Yang, H. Q., A. J. Przekwas. General strong conservation formulation of Navier-Stokes equations in nonorthogonal curvilinear coordinates, *AIAA Journal*, 1994, 32(5): 936-941.
- [18] Wikipedia, Curvilinear coordinates: https://en.wikipedia.org/wiki/Curvilinear_coordinates
- [19] Bellmann, R., 1997: Introduction to Matrix Analysis. ISBN: 0-89871-399-4
<https://books.google.com/book?id=QVCflvTPYE8C>.SIAM.
- [20] Hsu, W.-R., W. Y. Sun. A time-split, forward-backward numerical model for solving a nonhydrostatic and compressible system of equations. *Tellus*, 2001, 53A: 279-299.
- [21] Chen, S. H., W. Y. Sun. The applications of the multigrid method and a flexible hybrid coordinate in a nonhydrostatic model. *Mon. Wea. Rev.*, 2001, 129: 2660- 2676.
- [22] MacCall, B. T. 2006: Application of Reynolds' Stress Closure to the Stable Boundary Layer. Ph.D. Thesis, Dept. of Earth and Atmospheric Sciences, Purdue Univ., W. Lafayette, IN 47907.
- [23] Sun, W. Y., K. S. Yeh. A general semi-Lagrangian advection scheme employing forward trajectories. *J. R. Meteorol. Soc.*, , 1997, 123: 2463-2476
- [24] Sun, W. Y., O. M. Sun. Bernoulli Equation and Flow over a Mountain. *Geoscience Letters*, 2015, 2: 7.
DOI: [10.1186/s40562-015-0024-1](https://doi.org/10.1186/s40562-015-0024-1)
- [25] Sun, W. Y. Instability in Leapfrog and Forward-Backward Schemes: Part II: Numerical Simulation of Dam Break. *J. Computers and Fluids*, , 2011, 45: 70-76.